

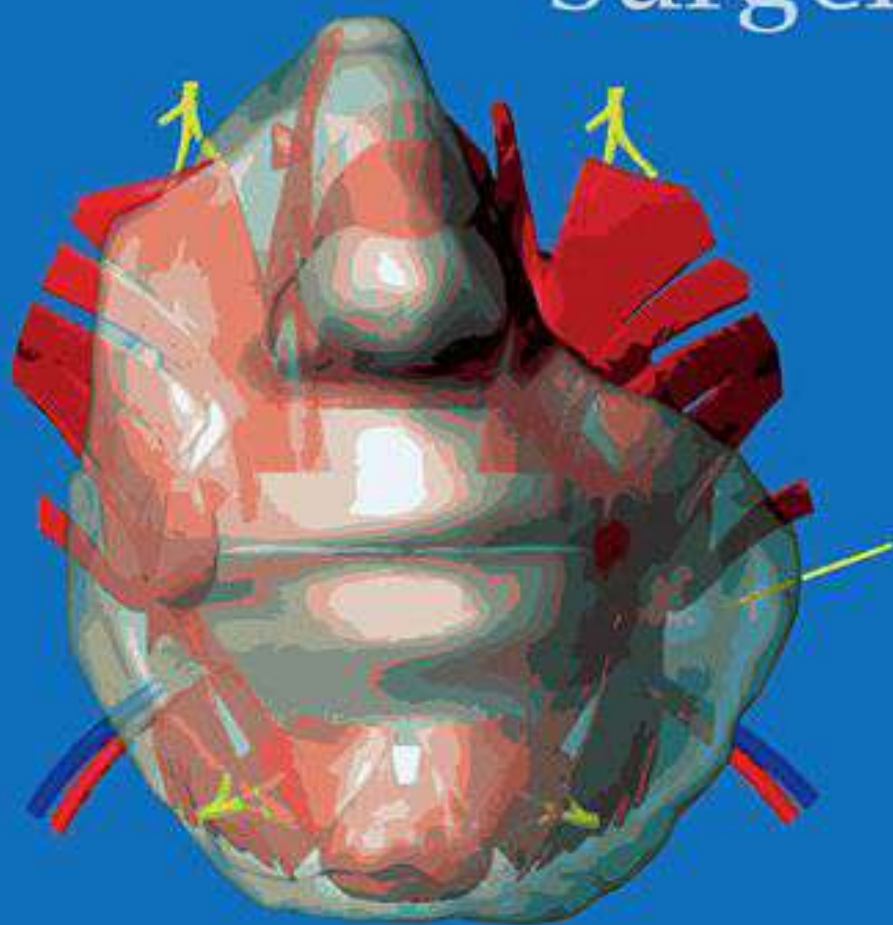


Volume 47 Issue 6

June 2019

ISSN 1010-5182

Journal of Cranio-Maxillo-Facial Surgery



Official Journal of the
European Association for Cranio-Maxillo-Facial Surgery

www.jcmfs.com



Quantification of the mandibular defect healing by micro-CT morphometric analysis in rats

T. Kustro^a, T. Kiss^b, D. Chernohorskyi^a, Y. Chepurnyi^{a,*}, Z. Helyes^{b,c}, A. Kopchak^a

^a Department of Stomatology, Bogomolets National Medical University, 13, T. Shevchenko Blvd, 01601, Kyiv, Ukraine

^b János Szentágothai Research Centre & Department of Pharmacology and Pharmacotherapy, Medical School, University of Pécs, Ifjúság útja 20, Pécs, H-7624, Hungary

^c PharmInVivo Ltd., Szondi Gy. u. 7, H-7629, Pécs, Hungary

ARTICLE INFO

Article history:

Paper received 1 July 2018

Accepted 19 September 2018

Available online 25 September 2018

Keywords:

Micro-CT

Bone regeneration

Bone mineral density

Bone volume

ABSTRACT

Purpose: The goal of this study was the evaluation of the bone tissue structural characteristics over the time course of mandibular defect healing using micro-CT technique, as well as determination of the inter-relationships between different micro-CT parameters used for assessment of the bone regeneration process and the patterns of their dynamic changes.

Materials and methods: The body and ramus of the mandible was exposed in 24 Wistar rats. A 2-mm full thickness bony defect was created. Animals were randomized into four groups, which were ended 3, 6, 12 and 24 weeks after operation. The mandible was excised and underwent micro-CT analysis. For statistical evaluation, the Mann–Whitney U test, polynomial or exponential regression and Spearman analysis were applied.

Results: The absolute volume of the bone regenerate increased from $1.69 \pm 0.53 \text{ mm}^3$ (3 weeks) to $3.36 \text{ mm}^3 \pm 0.56$ (6 months), as well as percentage of bone volume, increased significantly from $12.5 \pm 2.3\%$ at the 3-week term to $26.4 \pm 8.7\%$ at the 3-month term or $23.1 \pm 8.7\%$ at the 6-month term. Structural (trabecular) thickness gradually increased from $0.13 \pm 0.007 \text{ mm}$ at the 3-week term to $0.3 \pm 0.11 \text{ mm}$ at the 6-month term. The structural model index was 0.79 ± 0.46 in the early phase after trauma and then decreased to negative values.

Conclusion: The bone regeneration process was characterized by a significant increase ($p < 0.05$) in bone volume, percentage of bone volume, structural thickness and bone mineral density, and a decrease in bone surface-to-volume ratio and volume of pore space from the 3-week term to the 6-month term. These changes can be mathematically described by nonlinear exponential regression models.

© 2018 European Association for Cranio-Maxillo-Facial Surgery. Published by Elsevier Ltd. All rights reserved.

1. Introduction

Bone regeneration and remodeling has been extensively studied over the last decades, with an aim to develop new therapeutic approaches for fracture healing, treatment of the bone defects and osteointegration of implants. Significant progress in this field has been in with the development of new regenerative strategies, including guided tissue regeneration, tissue engineering, application of the stem cells and growth factors, advanced fixation devices and individualized implants (Giannoudis et al., 2005; Betz et al.,

2008; Schliephake et al., 2008; Zhang et al., 2010; Monaco et al., 2011; Kleinschmidt et al., 2013). However, repair of the large mandibular and maxillary defects, caused by congenital anomalies, trauma, infection, bisphosphonate-related osteonecrosis or tumor resections, as well as augmentation of the alveolar bone in cases of severe atrophy, remains a major challenge in oral and maxillo-facial surgery (Kaban and Glowacki, 1981; Kontogiorgos et al., 2011; Gomes and Fernandes, 2011; Beck-Broichsitter et al., 2015). Development of new approaches and techniques to enhance bone regeneration, substitute the lost tissue and control its remodeling require fundamental knowledge of mechanisms and patterns of bone regeneration processes.

Current research in this field is mainly based on animal models with surgically induced injuries of the bone, due to their

* Corresponding author. Bogomolets National Medical University, Stomatology department, Bilorusska street, 17 b, ap. 64, Kiev, Ukraine.

E-mail address: 80667788837@ukr.net (Y. Chepurnyi).

similarity to the trauma and recovery processes in maxillo-facial patients (Morgan et al., 2009; Jiang et al., 2009; Mashiba et al., 2011; Hassanein et al., 2012; Faot et al., 2015). These models are well established and include simple fracture models, ectopic bone formation and bone defect models (Histing et al., 2011; Kallai et al., 2011; Ning et al., 2017). The last ones were the most extensively used for analysis of the mandibular bone regeneration and can be divided, depending on their dimensions, into drill-hole models, which heal spontaneously, and critical-size bone defects, which require additional stimulation to be substituted with the newly formed bone (Kaban and Glowacki, 1981; Burg et al., 2000; Giannoudis et al., 2005; Betz et al., 2008; Gomes and Fernandes, 2011).

To quantify the bone growth within the defect in the course of regeneration process, different approaches have been used including histology, histomorphometry, immunohistochemistry, scanning electron microscopy, conventional radiology etc (Schliephake et al., 2008; Hassanein et al., 2012; Liu et al., 2016). However most of them were associated with specimen destruction and had strong limitation in three-dimensional (3-D) analysis of the regenerated microstructure (Jiang et al., 2009; Lin et al., 2012; Liu et al., 2016).

Recently, the use of micro-computed tomography (micro-CT) has offered the advantage of precise analysis of the healing process, bone microstructure and remodeling (Chappard et al., 2005; Swain and Xue, 2009; Bouxsein et al., 2010; Faot et al., 2015). It is a non-destructive method which provides a qualitative and quantitative assessment of bone volume and mineralization within an experimental bone defect, based on 3-D CT scans with high resolution (a voxel size between 0.3 and 100 μm) (Muller et al., 1998; Fajardo et al., 2002; Plachokova et al., 2007; Swain and Xue, 2009; Bissinger et al., 2015). Micro-CT can be used for visualization and structural evaluation of the newly formed bone by calculating the number of indexes, reflecting the bone microarchitecture and different sides of the regeneration process (Shefelbine et al., 2005; Schmidhammer et al., 2006; Morgan et al., 2009; Cuijpers et al., 2014; Beck-Broichsitter et al., 2015).

Several studies have used micro-CT to measure bone volume, bone volume fraction, and bone mineral density, as well as specific parameters of regenerate/callus structure for understanding the 3-D aspects of bone healing within the defects in different bones (Gabet et al., 2004; Midura et al., 2005; Morgan et al., 2009; Kallai et al., 2011; Faot et al., 2015). However, the mandible is a unique bone which carries a significant masticatory load. For this reason, the data obtained for other bones (e.g., calvarial defects) may not be applicable to the mandible (Kaban and Glowacki, 1981; Fontijn-Tekamp et al., 2000; Liu et al., 2016).

Most of the studies with mandibular defects investigated by micro-CT used the critical-size defect model in which bone regeneration was modulated by different therapeutic agents (Geiger et al., 2005; Ye et al., 2011; Hassanein et al., 2012; Manassero et al., 2013). There are only a few studies about the physiological regenerative potential of the mandibular bone, with certain contradictions concerning the interrelations between different micro-CT indexes over the course of bone healing. Clinical and biological significances of different micro-CT parameters in a baseline model, their prognostic value and influence on structure–function relationships in newly formed bone, as well as the patterns of its remodeling under the functional loads (Beck-Broichsitter et al., 2015) are also very different. Time-dependent patterns and regression models of bone regeneration developed for experimental fractures of the long bones cannot be successfully applied to the mandibular defect repair (den Boer et al., 1998; Shefelbine et al., 2005; Schmidhammer et al., 2006; Duvall et al., 2007; Beck-Broichsitter et al., 2015).

With the advancing of imaging technologies, rapid development of regenerative medicine and their wide application in oral and

maxillo-facial surgery, this knowledge has gained significant importance for both experimental research and clinical diagnostics (Swain and Xue, 2009; Morgan et al., 2009).

The aims of this study are to evaluate structural characteristics of the bone tissue over the time course of mandibular defect healing using micro-CT technique, as well as to determine the interrelationships between different micro-CT parameters used for assessment of the bone regeneration process and the patterns of their dynamic changes.

2. Materials and methods

2.1. Animals

Animal experiments were carried out in accordance with the European convention for the protection of animals used for experimental and other scientific purposes. The study was approved by Ethic commission in Bogomolets National Medical University. Three-month-old male Wistar rats were used for this study. A total of 24 male Wistar rats (taken from vivarium of Bogomolets National Medical University, Kyiv, Ukraine) with an average weight of 270 ± 30 g were used. The animals were kept in standard housing conditions and allowed free access to water and standard laboratory pellets.

2.2. Surgical procedure

The operation was performed under general anesthesia with an intraperitoneal ketamine (10% 100 mg/kg) injection. Articaine (Ultracaine DS, 3M ESPE; 0.5 ml) was additionally injected subcutaneously and into the masseter muscle for local anesthesia and control of bleeding. The animals were maintained under anesthesia during the entire surgical procedure. After local disinfection (Betadine 10%, Egis, Hungary), an incision in the skin was made, followed by masseter muscle dissection. The periosteum was elevated and the external surface of the mandibular body and ramus on the left side was exposed. A rotary drill (Medesy, Italy) with a diameter of 2 mm was used to create a round, full-thickness bony defect in the area of mandibular angle (Fig. 1). Such a diameter of the defect was chosen because, according to the literature, larger defects (3 mm or more) do not heal spontaneously and can be considered as “critical size defects” (Kaban and Glowacki, 1981; Beck-Broichsitter et al., 2015). The periosteum was placed in its original position, then the wound was closed with resorbable



Fig. 1. Surgical procedure: a circular defect with diameter 2-mm drilled in the area of the mandibular angle.

sutures (Vicryl®; Ethilon, Norderstedt, Germany). In the post-operative period, pain was relieved by Dexalgin (Berlin-chemie/Menarini pharma gmbh, Germany), 0.002 mg/g. For prophylaxis of infection development Ceftriaxone, 0.5 mg/g body weight, was injected intramuscularly for 1 day.

2.3. Study protocol

The animals were randomly divided into 4 equal groups with 6 animals in each. According to their group affiliation the animals were sacrificed after 3 weeks, 6 weeks, 3 months and 6 months, by an intraperitoneal overdose injection of Thiopental (Arterium, Ukraine). The hemimandible containing the body and ramus were explanted. The masticatory muscles were removed. The specimens were fixed in 4% phosphate-buffered formalin solution for further examination.

2.4. Micro-CT measurement and quantitative analysis of bone structure

Altogether 24 excised rat mandible samples were measured and analyzed. The mandibles were fixed to the bed in a spongy cylinder to locate them near to the spatial center of the gantry. Measurements were performed by a Skyscan 1176 micro-CT instrument and took approximately 70 min. The resolution of the images was 8.74 μm . Parameters of the source were set to 50 kV and 500 μA ; exposure time was 1000 ms.

After scanning, the raw images were reconstructed with the NRecon software, which was published by Bruker Inc. (Beck-Broichsitter et al., 2015). Ring artifact was set to 0, smoothing to 3 and beam hardening to 30%.

After reconstruction, the images were sent to CTAn software for further analysis also developed by Bruker Inc. Incisors were removed from the evaluation in order to clearly detect only the bone defects. The regions of interest (ROIs) were determined in the sagittal plane. A circular area with a 2-mm-wide diameter was set up at the first sagittal slice where the damage on the bone was clearly seen (Fig. 2A). The same was done on the contralateral side of the mandible also. These two ROIs on the two sides of the mandible formed a volume of interest (VOI) in three dimensions with a figure of a cylinder made by the CTAn software (Fig. 2B).

Every structure in this specified area was calculated for Hounsfield units (HU) proportional to bone mineral density (BMD), bone volume, bone surface and structural thickness, excluding the teeth. Two phantom rods were used for the calibration of the bone density measurements. BMD is defined as the volumetric density of calcium hydroxyapatite (CaHA) in terms of g/cm^3 . It is calibrated by means of phantoms with known BMD. It can refer to two slightly different measurements: to the density of a defined volume of bone plus soft tissue, as in trabecular (medullary) BMD, or to a density measurement restricted to within the volume of calcified bone tissue, such as cortical (volumetric) BMD. Hounsfield units are a standard unit of x-ray CT density, in which air and water are ascribed values of -1000 and 0 respectively. It has been found over several decades of CT imaging to be a useful general CT density calibration system (HU and BMD calibration in CT-analyzer; Bruker Inc.).

3-D reconstructions were also made from these datasets and colored to show the different bone mass values in the mandibles using the CTvox software developed by Bruker Inc (Fig. 3).

2.5. Statistical analysis

The micro-CT parameters of the bone regenerate were summarized as mean \pm standard deviations for each micro-CT index and each group. For analysis of the data, non-parametric statistics were used. The Mann–Whitney U test was used to

compare the changes in each parameter in different terms after trauma. The level of significance was set at $p < 0.05$. Statistical analyses were performed using SPSS software (IBM Corporation, Armonk, NY, USA). In order to evaluate the statistical connection between indexes and their time related dynamics linear, polynomial or exponential regression analysis were applied using OriginPro software. Spearman analysis was conducted to calculate the correlation coefficients between different micro-CT parameters.

3. Results

Macroscopic analysis revealed no signs of infection in all samples. However, in 5 cases, defects were not substituted with the newly formed bone. The percentage of bone volume within these samples was less than 0.2–0.4% in the early term and less than 5% in the late term after trauma. In all these cases, the defects were formed in the areas with thin bone represented only by cortical layer, and the general course of the impaired bone regeneration was like the critical size defects (Fig. 4). These cases were excluded from further analysis. In other samples the qualitative analysis of the bone regeneration process, based on micro-CT, revealed the following.

Three weeks after surgery, the defects were partially filled with the newly formed bone. It was represented by immature trabecular structure, more dense in the areas located near the defect borders. The margins of the defect area were clearly recognizable in all samples. The number and thicknesses of the bone structures as well as the number and dimensions of open or closed pores had significant topographic variability. It determines the certain extent of structural inhomogeneity of the regenerate in this term of observation.

Six weeks after surgery, the bone tissue of the regenerate became denser, trabecule increased in size, and in some areas the bone structure became more compact. The areas of the compact bone had an irregular shape and, at some locations, were integrated with the undamaged cortical layer of the mandible. At the same time, in all observations, it was possible to differentiate the boundaries of bone regenerate inside the defect, as its structure was significantly different from that of the intact bone.

Three months after surgery, the signs of bone remodeling were noted inside the defect with gradual restoration of the specific architectonics of the rat mandible in appropriate anatomical regions. The compact bone areas merged with each other and integrated with the surrounding bone to form a cortical layer the thickness and mineral density of which were less than in the intact cortical bone. The newly formed spongy bone was characterized by significant structural heterogeneity with the presence of large pores or dense/compacted areas and chaotic arrangement of the trabecular mesh. In general, the structure of the regenerate was different from the surrounding bone, although in this period of observation at individual sites it was quite difficult to determine the boundaries between them.

At the 6-month term, the samples differed slightly in the resultant pattern of bone regeneration and remodeling. In general, the margins of the defect area were not clearly recognizable. The restoration of the cortical layer continuity and a clear differentiation of the cortical and spongy bone layers were detected in all the samples. However, the architectonics and structure of the bone tissue inside the defect differed from those of the intact bone: the cortical layer was thinner, with less mineral density and was more porous. The spongy layer was characterized by a chaotic orientation of the bone structures. Their size, density, number and size of

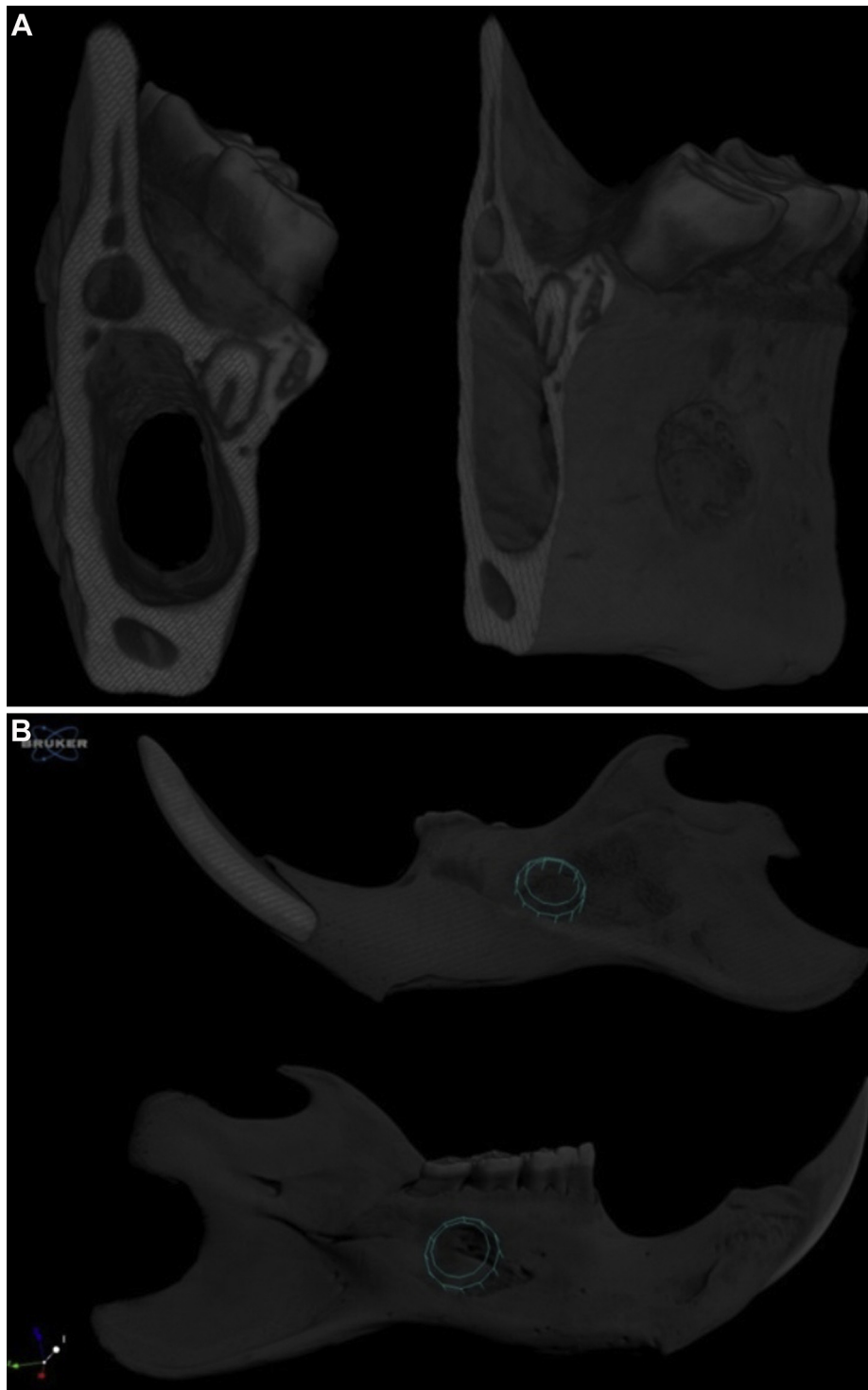


Fig. 2. Three-dimensional reconstruction of the rat mandible demonstrating the bone defect and healing after digitally removing the incisors (A) and the volumes of interest (VOI) for quantitative analysis (B).

pores did not match to the full extent the structure of the surrounding intact bone (Fig. 5).

Morphometric parameters calculated by a CT-analyzer in direct three dimensions based on surface rendered volume models of the defect are presented in Table 1. The total volume of the bone defects (VOI) ranged from 9.9 mm^3 to 16.7 mm^3 (mean $12.5 \pm 1.7 \text{ mm}^3$) with no statistical differences between groups. The absolute volume of the bone regenerate increased from $1.69 \pm 0.53 \text{ mm}^3$ (3

weeks) to $3.36 \text{ mm}^3 \pm 0.56$ (6 months), as well as the proportion of the VOI occupied by the newly formed bone structures (percentage of bone volume). This parameter increased significantly from $12.5 \pm 2.3\%$ at the 3-week term to $26.4 \pm 8.7\%$ or $23.1 \pm 8.7\%$ at the 6-month term. The percentage of bone volume is more precise in description of the defect substitution by the regenerating bone. Its increase was the most intensive during the first 3 weeks, then the rate of the new bone formation slowed and remained practically

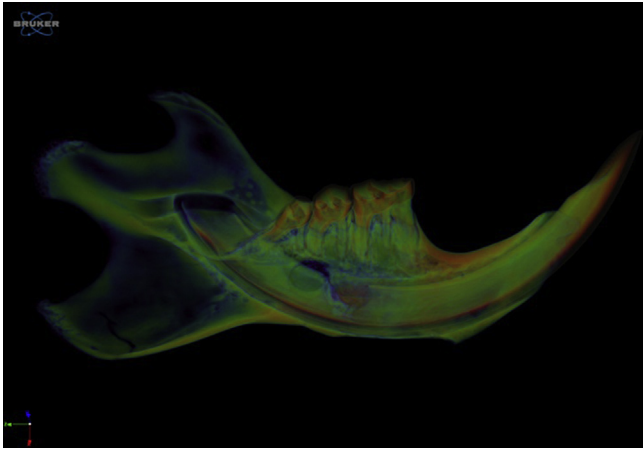


Fig. 3. Demonstrative picture of a 3-D reconstruction and artificial coloring of the rat mandible to visualize bone mineral density from blue (lowest) through green, yellow and red (highest).

stable after the 3-month term (Fig. 6). This process of mandibular defect substitution was well described by a non-linear (exponential fit) model (Fig. 7).

The bone remodeling in the course of regenerate maturing resulted in compaction and establishment of the more regular trabecular mesh; structural (trabecular) thickness gradually increased (Fig. 6) from 0.13 ± 0.007 mm at the 3-week term to 0.3 ± 0.11 mm at the 6-month term. Thickness distribution is a powerful means of characterizing the shape of a complex structure. The most intensive rate of trabecular thickness changes was observed between 3 and 6 weeks after trauma. There were no significant differences in bone surface (the surface area of all the bone objects within the VOI), but the bone surface/volume ratio significantly decreased at the 6-week term and then stabilized at practically the same level. Surface-to-volume ratio is considered a useful parameter for characterizing the thickness and complexity of structures. Regression analysis for this index, reflecting the bone remodeling process, revealed evidence for a highly significant exponential ($R^2 = 0.78$, $p < 0.01$) statistical association (Fig. 7).

There were no significant changes in such morphometric parameters as structural separation and structural linear density during the course of the bone defect healing. At the same time there was a tendency toward a slight increase in degree of anisotropy within the VOI over the course of bone regenerate formation and remodeling; however it was not significant for this number of observations. The structural model index (SMI), which indicates the prevalence of the rod-like or plate-like structures within the VOI (Hildebrand and Ruegsegger, 1997), was the highest in the early term after trauma (mean value 0.79 ± 0.46) and then decreased to the negative values. In normal bone, a value of 3 indicates a rod-like structure, and a value of 0 indicates a plate-like structure; but in regenerated mandibular bone, because of increased bone remodeling, trabecular plates may be perforated and connecting rods dissolved, so traditional procedures, which are based on a fixed model type, might lead to questionable results (Kontogiorgos et al., 2011), such as negative SMI values observed in at 6-week and 3-month terms.

Fractal dimension, which is an indicator of surface complexity of an object and quantifies how that object's surface fills space, demonstrated no significant changes over the course of the bone regeneration.

The bone density inside the defect increased according to the non-linear law with the most intensive dynamics in 3-week and 6-week terms.

The analysis of such indexes as the number of objects and the number and volume of pores showed that such indexes for mandibular bone regeneration are less informative than for normal trabecular bone analysis, due to the high individual variability. In general there was a tendency toward a decrease in the number of objects over time, reflecting the process of bone compaction and restoration of its functional integrity. However the changes in this index were insignificant for the number of observations included in the study. The closed pores were few in number and their volume was negligibly small. The total porosity of the regenerate was absolutely determined by open pore spaces. This index decreased significantly in late terms after trauma and correlated with an increase in percentage of bone volume.

4. Discussion

The study of the mandibular regeneration, specification of the patterns for bone tissue proliferation and remodeling, and mathematical description of the time-dependent changes of the bone architecture in the injured zones has great importance for treatment planning and prognosis in bone reconstructive and orthognathic surgery, oral implantology and facial trauma management. The volume of newly formed bone, its mineral density, structural integrity, morphological characteristics of the trabecular mesh and compact bone areas determine the bone quality, its mechanical properties and the long-term success of the surgical interventions (den Boer et al., 1998; Shefelbine et al., 2005; Bauer et al., 2006; Morgan et al., 2009).

Currently micro-CT is the gold standard for assessing BMD and bone microstructural features. It is considered to be a proper method for experimental evaluation of the bone architecture and structural morphology under various pathologic conditions (Swain and Xue, 2009; Boussein et al., 2010; Faot et al., 2015; Bissinger et al., 2015). It has significant limitations in comparison with histomorphometric study, as it has no possibility to analyze the cell proliferation and differentiation, microcirculation and vascularization inside the bone, rate of mineral apposition and bone remodeling. However it provides highly informative and precise imaging data for 3-D quantitative morphometric analysis of the bone structure. The advantages of micro-CT application are nondestructive assessment of internal and external bone morphology, high resolution and accuracy (Muller et al., 1998; Fajardo et al., 2002; Chappard et al., 2005; Cuijpers et al., 2014; Liu et al., 2016).

Micro-CT is also widely used for pre-clinical evaluation of the bone plastic materials and scaffolds for tissue engineering, their architecture, degradation and remodeling, as well as the healing capability of bone regenerative materials and new bone formation within the scaffold or mineral matrix (Burg et al., 2000; Geiger et al., 2005; Morgan et al., 2009). Such studies are performed in the standard animal models, and for proper interpretation of the obtained results there is a need for good understanding of healing patterns in mandibular bone and changes in the main morphological parameters in the normal course of bone regeneration (Midura et al., 2005; Jiang et al., 2009; Li et al., 2015). The mathematical description of these changes and associations between parameters that reflect different aspects of the regeneration process is also a problem of great clinical significance.

The number of micro-CT parameters and indexes are used to study the bone morphology in long bones either in normal or in pathological conditions (for example, in osteoporosis). Their referent values and biological relevance, as well as correlations with quantitative histological and histomorphometric indexes, are

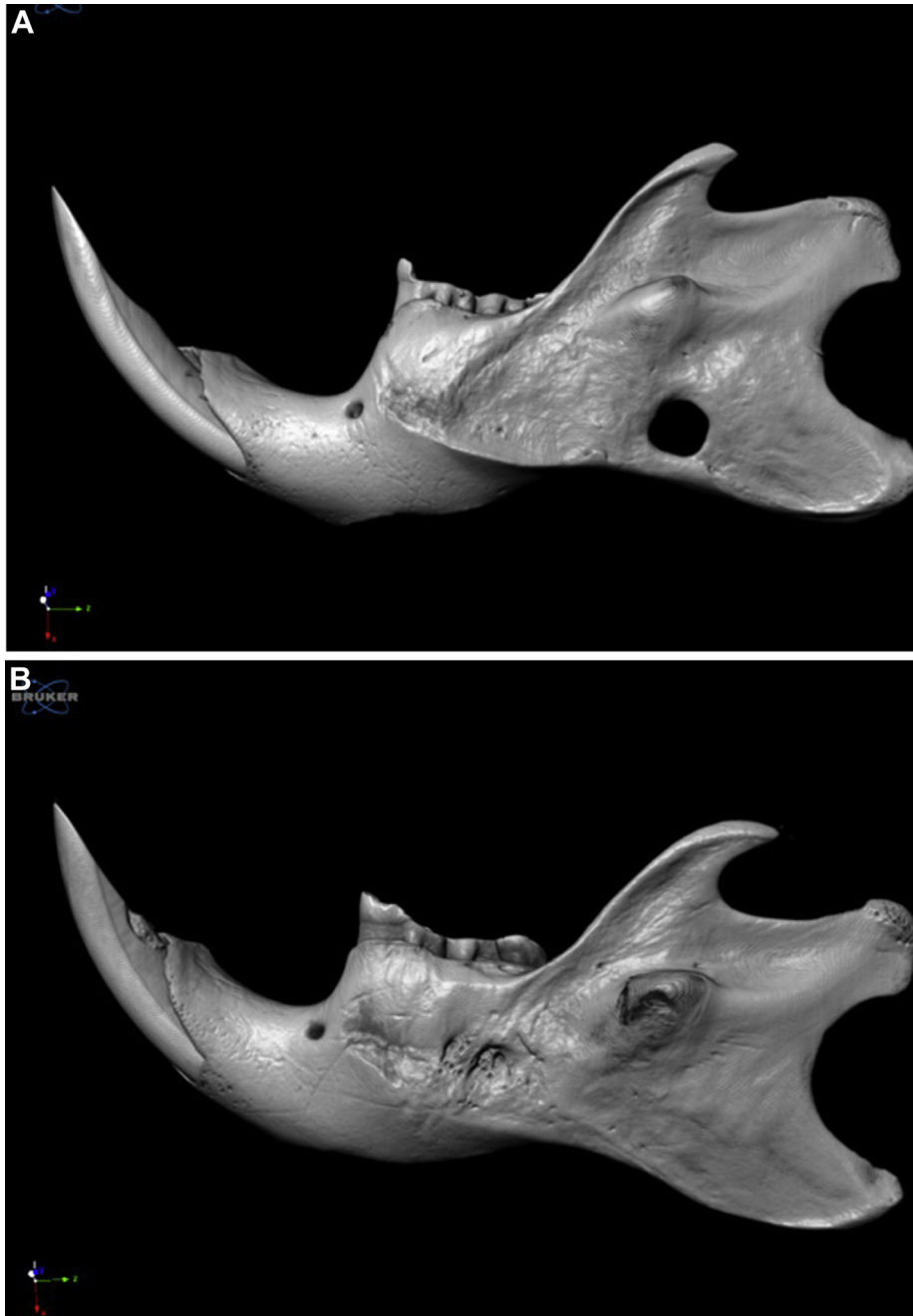


Fig. 4. Demonstrative 3-D reconstruction pictures of (A) impaired bone regeneration 3 months after surgery with no signs of bone defect substitution, and (B) the normal course of the bone regeneration 3 months after surgery, in which the bone defect is substituted by the newly formed bone.

well established for the long bones in experimental animal studies and human bone biopsies (Fajardo et al., 2002; Reddy and Lakshmana, 2003; Francisco et al., 2011; Kallai et al., 2011).

However, the values of micro-CT morphometrical parameters and their dynamics in the normal course of bone regeneration after traumatic injury have rarely been reported (den Boer et al., 1998; Schmidhammer et al., 2006; Morgan et al., 2009). The mandible is significantly different from long bones in its architecture, anatomical shape and loading conditions. Due to the specific mechanical load and embryogenesis, the cortical-to-trabecular bone ratio in the rat mandible is higher than in other bones (e.g., long bones). Stereology-based comparison of the trabecular bone structures in the mandible or tibia by

histological and micro-CT methods have shown significant differences in qualitative morphometrical parameters, reflecting the differences in micro-architecture of the mandibular bone, so observations in other bones may not be transferable to the mandible (Liu et al., 2016). There are only a few studies in which the impact of surgical interventions or exogenic factors on the bone healing or regeneration in the mandibular bone was investigated (Kontogiorgos et al., 2011; Faot et al., 2015; Beck-Broichsitter et al., 2015).

In present study, micro-CT was capable of visualizing the new bone formation inside the mandibular defect and 3-D changes in regenerate structure over the course of the bone healing process with a high level of accuracy. Among the numerous parameters that

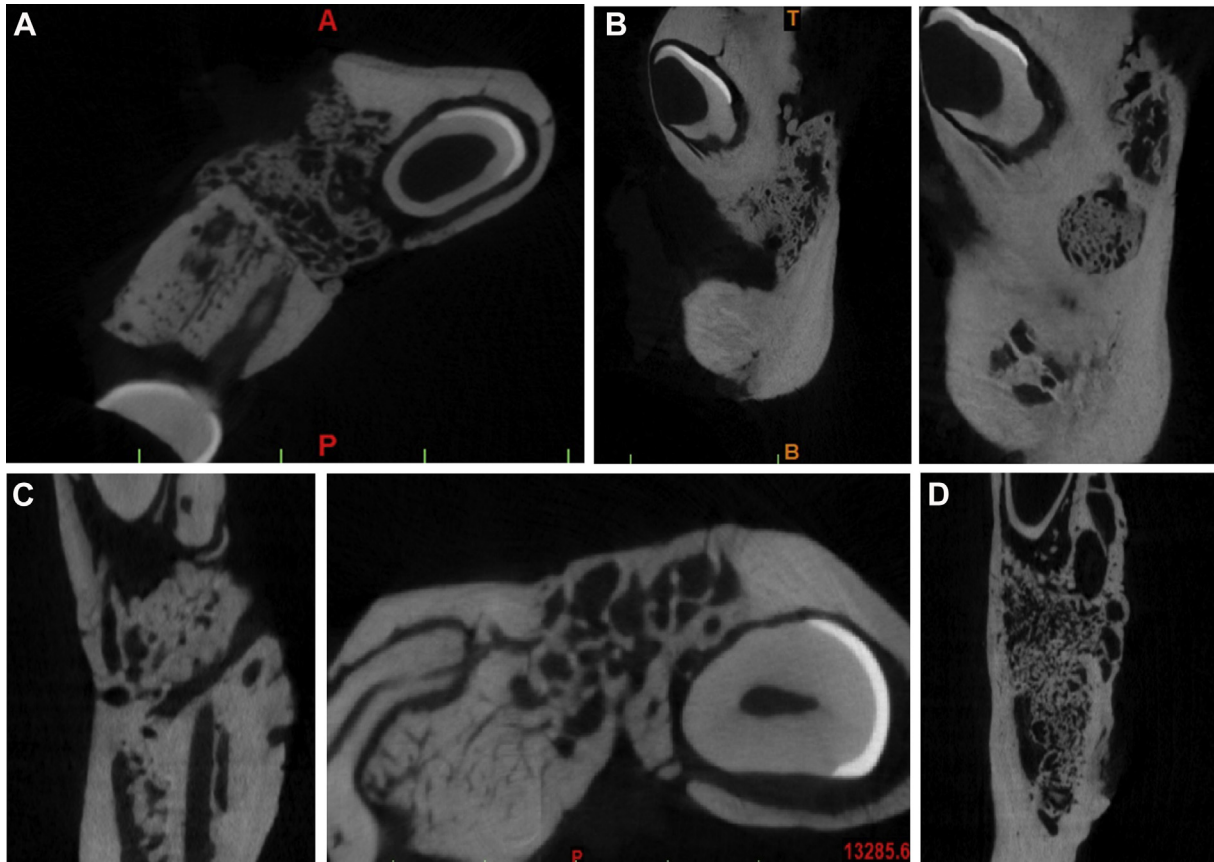


Fig. 5. Micro-CT slices passing through the bone defects, filled with newly formed bone. (A) 3-Week term; (B) 6-week term; (C) 3-month term; (D) 6-month term.

Table 1
Micro-CT morphometric parameters of the bone regenerate in 3-D analysis.

Parameter	3-D integrated analysis of all objects in VOI (mean + SD)			
	3 weeks	6 weeks	3 months	6 months
Number of samples	4	4	5	5
Total bone volume, mm ³	1.69 ± 0.53	2.03 ± 0.89	3.3 ± 1.18 ^a	3.36 ± 0.56 ^a
Percent bone volume, %	12.5 ± 2.3	16.6 ± 6.7	26.4 ± 8.6 ^a	23.1 ± 8.6 ^a
Bone surface, mm ²	46.7 ± 12.8	30.3 ± 10.7	44.6 ± 8.6	45.1 ± 17.5
Bone surface/volume ratio, mm ⁻¹	27.9 ± 1.3	15.5 ± 2.3 ^a	14.2 ± 2.7 ^a	13.4 ± 4.6 ^a
Bone surface density	3.5 ± 0.5	2.5 ± 0.7 ^a	3.6 ± 0.7	2.8 ± 0.5
Structure thickness, mm	0.13 ± 0.007	0.2 ± 0.016 ^a	0.25 ± 0.048 ^a	0.3 ± 0.11 ^a
Structure separation	0.98 ± 0.07	1.11 ± 0.22	0.86 ± 0.12	1.1 ± 0.29
Structure lineal density	0.96 ± 0.14	0.7 ± 0.24	1.02 ± 0.2	0.77 ± 0.17
Degree of anisotropy	1.7 ± 0.37	1.8 ± 0.2	1.8 ± 0.35	2.2 ± 0.56
Fractal dimension	2.19 ± 0.093	2.12 ± 0.3	2.27 ± 0.089	2.24 ± 0.1
Bone mineral density, g/cm ³	0.17 ± 0.02	0.26 ± 0.01 ^a	0.28 ± 0.02 ^a	0.3 ± 0.08 ^a
Number of objects	59.2 ± 27.2	37.25 ± 37	15.2 ± 14.6	20.4 ± 11.6
Number of closed pores	15.8 ± 10.9	16.75 ± 8.61	10 ± 6.32	10 ± 5.66
Volume of closed pores, x 10 ⁻³ mm ³	0.9 ± 0.5	1.9 ± 0.8	2.4 ± 3	5.7 ± 6
Closed porosity, %	0.05 ± 0.02	0.1 ± 0.01 ^a	0.07 ± 0.07	0.18 ± 0.2
Volume of open pores, mm ³	11.6 ± 1.6	9.98 ± 0.8	9.15 ± 1.1	13.1 ± 8.1
Open porosity, %	87.5 ± 2.3	83.3 ± 6.73	73.5 ± 8.6 ^a	76.9 ± 8.6 ^a
Connectivity	391.5 ± 167	93.8 ± 51.3 ^a	137.6 ± 37 ^a	187.6 ± 224
Connectivity density	28.5 ± 8.9	7.6 ± 3.6 ^a	11.2 ± 3.6 ^a	9.3 ± 7.84 ^a

^a Differences with 3-week term are significant ($p < 0.05$ by Mann–Whitney U test).

can be used to describe trabecular bone microarchitecture and cortical bone morphology (Shefelbine et al., 2005; Morgan et al., 2009; Bouxsein et al., 2010; Kallai et al., 2011), only a few appear to be useful for characterization of the bone healing processes. The most informative indexes which describe the course of the bone regeneration have been total bone volume, percentage of bone volume, bone surface-to-volume ratio, structural thickness, bone mineral density and structural connectivity.

Such indexes as bone surface density, structural separation, structural linear density, structural model index, fractal dimension, surface convexity index and degree of anisotropy, which were previously used in describing trabecular bone microarchitecture (Müller et al., 1996; Bouxsein et al., 2010; Faot et al., 2015; Liu et al., 2016), appeared to be non-informative in mandibular regeneration studies. As shown in previous studies, such factors as trabecular thickness, connectivity, anisotropy and special complexity of the trabecular mesh as well as the bone mineral density are important determinants of bone strength and stiffness that are important for the functional capacity of the bone under specific loading conditions (Ulrich et al., 1999; Shefelbine et al., 2005; Gardner et al., 2008; Morgan et al., 2009).

The bone healing process was characterized by a gradual increase in bone volume, structural thickness and bone mineral density, and a decrease in bone surface-to-volume ratio and volume of pore space. Areas of new bone formation were clearly detectable 3 weeks after operation, with a significant increase in bone volume until the end of the study in a 3-D evaluation. The irregular trabecular mesh of thin bone plates which filled the defect in the early stages of the bone regeneration (3 and 6 weeks) became more compact, underwent significant remodeling and increased in

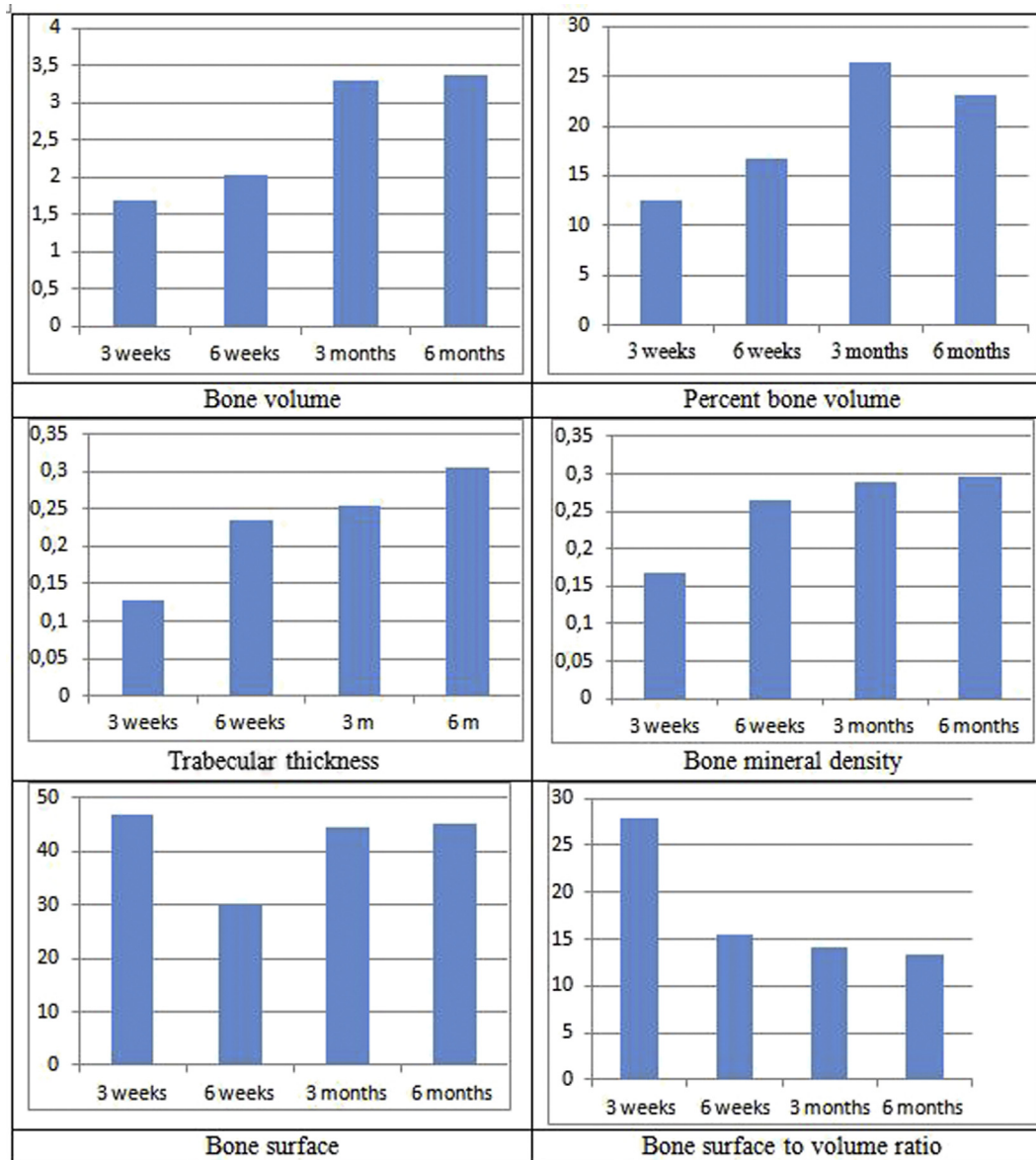


Fig. 6. Dynamics of the micro-CT parameter measurement in 3-D evaluation.

mineral density up to the 6-month term. These changes reflect the normal course of the bone healing aimed at restoration of the original bone shape, volume and quality.

However, even in late terms after trauma (i.e., 6 months), the structure of the bone regenerate did not exactly match the architectonics of the surrounding intact bone. Kontogiorgos came to the same conclusion regarding mineral density and bone volume fraction between mandibular regenerated and native bone after 12 and 18 weeks of consolidation. The author showed that native bone was denser because of a thick outer layer of cortical bone that was not formed in the regenerate in these terms, but the regenerate showed a significantly higher number of thicker trabecule, which contributed to its mechanical properties to withstand mastication loads.

The general course of the bone regeneration in our study also corresponded to the previous results of the histomorphometric studies in animal models with the same terms of observation (Cope and Samchukov, 2000). However, the obtained data helps to quantify the bone regenerate more precisely and gives a

comprehensive view on the 3-D morphology of new bone formation.

It was demonstrated that the changes in the main micro-CT parameters are well described by non-linear exponential models. The linear regression models proposed by some authors (Umoh et al., 2009; Beck-Broichsitter et al., 2015) are valid only for early terms after trauma and can be considered only as a segment of more general consistent pattern. The regression models obtained in the study represent the normal course of the bone regeneration and can be used for prognosis in both experimental and clinical studies. In the future, with further improvement of conventional CT and software for CT data analysis and visualization, it will be possible to obtain more accurate and reliable quantitative data on bone regeneration in patients who have undergone operation on facial bones.

The present study has several limitations. The number of samples included in the final analysis was relatively small (4–6 animals in each group), with marked individual variability for some parameters. The main findings cannot be directly transferred to

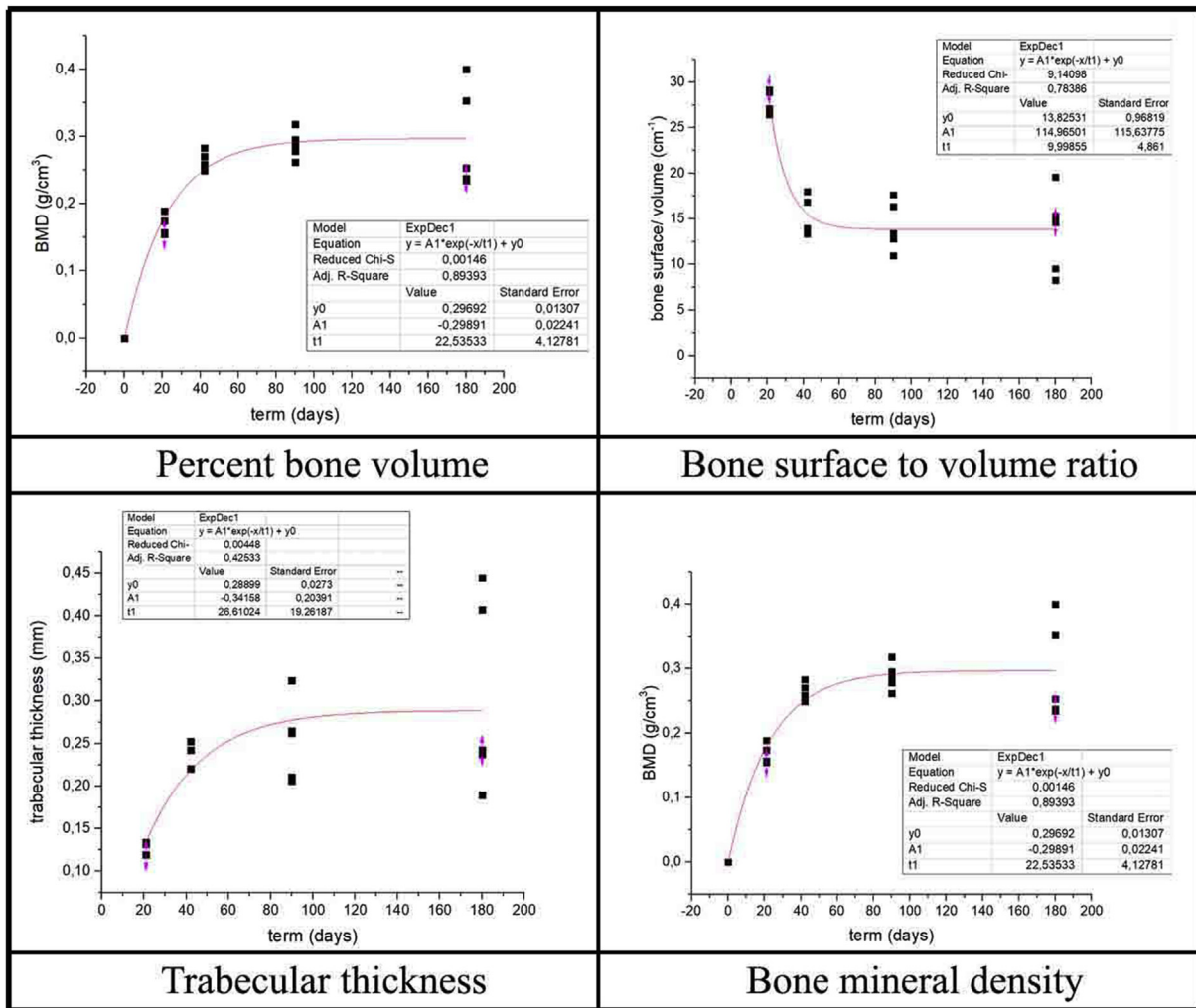


Fig. 7. Exponential regression analysis of the micro-CT parameters and their dynamics in postoperative follow-up.

humans, as there are significant differences in functional anatomy and increased bone turnover in rats in comparison to those in humans. All rats were sacrificed before micro-CT scanning, so there was no possibility for longitudinal study of the bone microstructural changes in each animal during all the observation terms. There were some topographic differences in the location of the defects, which may have influenced the course of the bone regeneration process. However, in all cases such differences were significant (bone defects, located in the incorrect position within the ramus were excluded from the study). The micro-CT scanning of the samples was performed without any histologic or biomechanical evaluation of the bone regenerate, which may be important for the proper interpretation of the obtained results, and can be the subject for further investigations.

5. Conclusion

Micro-CT analysis proved to be an informative and highly accurate method for 3-D morphometrical analysis and quantitative characterization of bone microstructure in mandibular bone regeneration. The bone regeneration process was characterized by a significant increase ($p < 0.05$) in bone volume, percentage of bone volume, structural thickness and bone mineral density, and by a decrease in bone surface-to-volume ratio and volume of pore space from the 3-week term to the 6-month term. These changes can be mathematically described by non-linear exponential regression

models. The general course of the regeneration process resulted in adaptive changes in 3-D morphology of the bone tissue, but even in late terms after trauma (i.e., at 6 months), the structure of the bone regenerate did not exactly match the architectonics of the surrounding intact bone. The results contribute to a better understanding of the postoperative healing process and can be used for diagnostics, treatment planning and prognosis in patients with facial bone pathology.

Ethical approval

All applicable international, national, and institutional guidelines for the care and use of animals were followed.

Authors' Roles

Andriy Kopchak, Yurii Chepurnyi, Kustro Tatiana – Conception and design, analysis and interpretation of data, drafting the article.

Yurii Chepurnyi, Denis Chernogorskiy, Tatiana Kustro, Tamas Kiss – Data collection, analysis and interpretation of data.

Andriy Kopchak, Zsuzsanna Helyes – critically revising the article, study supervision.

Acknowledgements

The project was supported by Hungarian grants SZRC Core Facility Development EFOP-3.6.1-16-2016-00004 and STAY ALIVE GINOP-2.3.2-15-2016-00048 – “Excellence of R+D Strategic

Centres: Improving the severity and lethality parameters of life-threatening diseases from a translational approach”.

References

- Bauer J, Kohlmann S, Eckstein F, Mueller D, Lochmuller E, Link T: Structural analysis of trabecular bone of the proximal femur using multislice computed tomography: a comparison with dual X-ray absorptiometry for predicting biomechanical strength in vitro. *Calcif Tissue Int* 78: 78–89. <https://doi.org/10.1007/s00223-005-0070-3>, 2006
- Beck-Broichsitter BE, Garling A, Koehne T, Barvencik F, Smeets R, Mehl C, et al: ST3D-tracking the regenerative potential of the mandible with micro-CTs. *Oral Maxillofac Surg* 19(1): 29–35. <https://doi.org/10.1007/s10006-014-0443-8>, 2015
- Betz VM, Betz OB, Harris MB, Vrahas MS, Evans CH: Bone tissue engineering and repair by gene therapy. *Front Biosci* 13(3): 833–841, 2008 10.2741/2724
- Bissinger O, Kirschke JS, Probst FA, Stauber M, Wolff KD, Haller B, et al: A micro-CT vs. whole body multirow detector CT for analysing bone regeneration in an animal model. *PLoS One* 11(11): e0166540. <https://doi.org/10.1371/journal.pone.0166540>, 2015
- Bouxsein ML, Boyd SK, Christiansen BA, Guldberg RE, Jepsen KJ, Muller R: Guidelines for assessment of bone microarchitecture in rodents using micro-computed tomography. *J Bone Miner Res* 25: 1468–1486. <https://doi.org/10.1002/jbmr.141>, 2010
- Burg KJ, Porter S, Kellam JF: Biomaterial developments for bone tissue engineering. *Biomaterials* 21(23): 2347–2359. [https://doi.org/10.1016/s0142-9612\(00\)00102-2](https://doi.org/10.1016/s0142-9612(00)00102-2), 2000
- Chappard D, Retailleau-Gaborit N, Legrand E, et al: Comparison insight bone measurements by histomorphometry and microCT. *J Bone Miner Res* 20: 1177–1184. <https://doi.org/10.1359/jbmr.050205>, 2005
- Cope JB, Samchukov ML: Regenerate bone formation and remodeling during mandibular osteodistraction. *Angle Orthod* 70: 99–111. [https://doi.org/10.1043/0003-3219\(2000\)070<0099:RBFARD>2.0.CO;2](https://doi.org/10.1043/0003-3219(2000)070<0099:RBFARD>2.0.CO;2), 2000
- Cuijpers VM, Jaroszewicz J, Anil S, Al Farraj Aldosari A, Walboomers XF, Jansen JA: Resolution, sensitivity, and in vivo application of high-resolution computed tomography for titanium-coated polymethyl methacrylate (PMMA) dental implants. *Clin Oral Implants Res* 25(3): 359–365. <https://doi.org/10.1111/clr.12128>, 2014
- den Boer FC, Bramer JA, Patka P, Bakker FC, Barentsen RH, Feilzer AJ, et al: Quantification of fracture healing with three-dimensional computed tomography. *Arch Orthop Trauma Surg* 117: 345–350. <https://doi.org/10.1007/s004020050263>, 1998
- Duvall CL, Taylor WR, Weiss D, Wojtowicz AM, Guldberg RE: Impaired angiogenesis, early callus formation, and late stage remodeling in fracture healing of osteopontin-deficient mice. *J Bone Miner Res* 22: 286–297. <https://doi.org/10.1359/jbmr.061103>, 2007
- Fajardo RJ, Ryan TM, Kappelman J: Assessing the accuracy of high-resolution X-ray computed tomography of primate trabecular bone by comparisons with histological sections. *Am J Phys Anthropol* 118: 1–10. <https://doi.org/10.1002/ajpa.10086>, 2002
- Faot F, Chatterjee M, de Camargos GV, Duyck J, Vandamme K: Micro-CT analysis of the rodent jaw bone micro-architecture: a systematic review. *Bone Rep* 2: 14–24. <https://doi.org/10.1016/j.bonr.2014.10.005>, 2015 eCollection 2015 Jun
- Fontijn-Tekamp FA, Slagter AP, Van Der Bilt A, Van'T Hof MA, Witter DJ, Kalk W, et al: Biting and chewing in overdentures, full dentures, and natural dentitions. *J Dent Res* 79(7): 1519–1524. <https://doi.org/10.1177/00220345000790071501>, 2000
- Francisco JJ, Yu Y, Oliver RA, Walsh WR: Relationship between age, skeletal site, and time postovariectomy on bone mineral and trabecular microarchitecture in rats. *J Orthop Res* 29(2): 189–196. <https://doi.org/10.1002/jor.21217>, 2011
- Gabet Y, Muller R, Regev E, Sela J, Shteyer A, Salisbury K, et al: Osteogenic growth peptide modulates fracture callus structural and mechanical properties. *Bone* 35: 65–73. <https://doi.org/10.1016/j.bone.2004.03.025>, 2004
- Gardner MJ, van der Meulen MC, Demetropoulos D, Wright TM, Myers ER, Bostrom MP: In vivo cyclic axial compression affects bone healing in the mouse tibia. *J Orthop Res* 24: 1679–1686. <https://doi.org/10.1002/jor.20230>, 2008
- Geiger F, Bertram H, Berger I, Lorenz H, Wall O, Eckhardt C, et al: Vascular endothelial growth factor gene-activated matrix (VEGF165-GAM) enhances osteogenesis and angiogenesis in large segmental bone defects. *J Bone Miner Res* 20: 2028–2035. <https://doi.org/10.1359/jbmr.050701>, 2005
- Giannoudis PV, Dinopoulos H, Tsiroidis E: Bone substitutes: an update. *Injury* 36: 20–S27. <https://doi.org/10.1016/j.injury.2005.07.029>, 2005
- Gomes PS, Fernandes MH: Rodent models in bone-related research: the relevance of calvarial defects in the assessment of bone regeneration strategies. *Lab Anim* 45(1): 14–24. <https://doi.org/10.1258/la.2010.010085>, 2011 Epub 2010 Dec 14
- Hassanein AH, Arany PR, Couto RA, Clune JE, Glowacki J, Rogers GF, et al: Cranial particulate bone graft ossifies calvarial defects by osteogenesis. *Plast Reconstr Surg* 129(5): 796e–802e. <https://doi.org/10.1097/PRS.0b013e31824a2bdd>, 2012
- Hildebrand T, Rueggsegger P: Quantification of bone microarchitecture with the structure model index. *Comput Methods Biomech Biomed Eng* 1: 15–23. <https://doi.org/10.1080/0149573970893692>, 1997
- Histing T, Garcia P, Holstein JH, Klein M, Matthys R, Nuetzi R, et al: Small animal bone healing models: standards, tips, and pitfalls results of a consensus meeting. *Bone* 49: 591–599. <https://doi.org/10.1016/j.bone.2011.07.007>, 2011 Epub 2011 Jul 19
- Jiang X, Zhao J, Wang S, Sun X, Zhang X, Chen J, et al: Mandibular repair in rats with premineralized silk scaffolds and BMP-2-modified bMSCs. *Biomaterials* 30(27): 4522–4532. <https://doi.org/10.1016/j.biomaterials.2009.05.021>, 2009 Epub 2009 Jun 6
- Kaban LB, Glowacki J: Induced osteogenesis in the repair of experimental mandibular defects in rats. *J Dent Res* 60(7): 1356–1364. <https://doi.org/10.1177/00220345810600071201>, 1981
- Kallai I, Mizrahi O, Tawackoli W, Gazit Z, Pelled G, Gazit D: Microcomputed tomography-based structural analysis of various bone tissue regeneration models. *Nat Protoc* 6(1): 105–110. <https://doi.org/10.1038/nprot.2010.180>. Epub 2011 Jan 6, 2011
- Kleinschmidt K, Ploeger F, Nickel J, Glockenmeier J, Kunz P, Richter W: Enhanced reconstruction of long bone architecture by a growth factor mutant combining positive features of GDF-5 and BMP-2. *Biomaterials* 34: 5926–5936. <https://doi.org/10.1016/j.biomaterials.2013.04.029>, 2013
- Kontogiorgos E, Elsalanty ME, Zapata U, Zakhary I, Nagy WW, Dechow PC, et al: Three-dimensional evaluation of mandibular bone regenerated by bone transport distraction osteogenesis. *Calcif Tissue Int* 89(1): 43–52. <https://doi.org/10.1007/s00223-011-9492-2>, 2011
- Li Y, Chen SH, Li L, Qin L: Bone defect animal models for testing efficacy of bone substitute biomaterials. *J Orthop Trans* 3(3). <https://doi.org/10.1016/j.jot.2015.05.002>, 2015 95–10
- Lin CY, Chang YH, Kao CY, Lu CH, Sung LY, Yen TC: Augmented healing of critical-size calvarial defects by baculovirus-engineered MSCs that persistently express growth factors. *Biomaterials* 33(14): 3682–3692. <https://doi.org/10.1016/j.biomaterials.2012.02.007>, 2012
- Liu H, Li W, Liu YS, Zhou YS: Bone micro-architectural analysis of mandible and tibia in ovariectomized rats: a quantitative structural comparison between undecalcified histological sections and micro-CT. *Bone Joint Res* 5(6): 253–262. <https://doi.org/10.1302/2046-3758.56.2000565> PMID: PMC4957176, 2016
- Manassero M, Viateau V, Matthey R, Descheppe M, Vallefuoco R, Bensidhoum M, et al: A novel murine femoral segmental critical-sized defect model stabilized by plate osteosynthesis for bone tissue engineering purposes. *Tissue Eng Part C Methods* 19(4): 271–280. <https://doi.org/10.1089/ten.TEC.2012.0256>, 2013 Epub 2012 Oct 19
- Mashiba T, Iwata K, Komatsubara S, Manabe T: Animal models for bone and joint disease. *Animal fracture model and fracture healing process*. *Clin Calcium* 21: 235–241, 2011 <https://doi.org/10.1111/10111102235241>
- Midura RJ, Ibiwoye MO, Powell KA, Sakai Y, Doehring T, Grabner MD, et al: Pulsed electromagnetic field treatments enhance the healing of fibular osteotomies. *J Orthop Res* 23: 1035–1046. <https://doi.org/10.1016/j.orthres.2005.03.015>, 2005
- Monaco E, Bionaz M, Hollister SJ, Wheeler MB: Strategies for regeneration of the bone using porcine adult adipose-derived mesenchymal stem cells. *Theriogenology* 75(8): 1381–1399. <https://doi.org/10.1016/j.theriogenology.2010.11.020>, 2011
- Morgan EF, Mason ZD, Chien KB, Pfeiffer AJ, Barnes GL, Einhorn TA, et al: Micro-computed tomography assessment of fracture healing: relationships among callus structure, composition, and mechanical function. *Bone* 44: 335–344. <https://doi.org/10.1016/j.bone.2008.10.039>, 2009
- Müller R, Koller B, Hildebrand T, et al: Resolution dependency of microstructural properties of cancellous bone based on three-dimensional mu-tomography. *Technol Health Care* 4: 113–119. <https://doi.org/10.3233/thc-1996-4112>, 1996
- Muller R, Van Campenhout H, Van Damme B, Van Der Perre G, Dequeker J, Hildebrand T, et al: Morphometric analysis of human bone biopsies: a quantitative structural comparison of histological sections and micro-computed tomography. *Bone* 23: 59–66. [https://doi.org/10.1016/s8756-3282\(98\)00068-4](https://doi.org/10.1016/s8756-3282(98)00068-4), 1998
- Ning B, Zhao Y, Buza J, Li W, Wang W, Jia T: Surgically-induced mouse models in the study of bone regeneration: current models and future directions. *Mol Med Rep* 15(3): 1017–1023. <https://doi.org/10.3892/mmr.2017.6155>, 2017
- Plachokova AS, van den Dolder J, Stoeltinga PJ, Jansen JA: Early effect of platelet-rich plasma on bone healing in combination with an osteoconductive material in rat cranial defects. *Clin Oral Implants Res* 18(2): 244–251. <https://doi.org/10.1111/j.1600-0501.2006.01327.x>, 2007
- Reddy NP, Lakshmana M: Prevention of bone loss in calcium deficient ovariectomized rats by OST-6, a herbal preparation. *J Ethnopharmacol* 84(2): 259–264. [https://doi.org/10.1016/s0378-8741\(02\)00325-2](https://doi.org/10.1016/s0378-8741(02)00325-2), 2003
- Schliephake H, Weich HA, Dullin C, Gruber R, Frahe S: Mandibular bone repair by implantation of rhBMP-2 in a slow release Carrier of polylactic acid an experimental study in rats. *Biomaterials* 29: 103–110. <https://doi.org/10.1016/j.biomaterials.2007.09.019>, 2008
- Schmidhammer R, Zandieh S, Mittermayr R, Pelinka LE, Leixnering M, Hopf R, et al: Assessment of bone union/nonunion in an experimental model using micro-computed technology. *J Trauma* 61: 199–205. <https://doi.org/10.1097/01.ta.0000195987.57939.7e>, 2006
- Shefelbine SJ, Simon U, Claes L, Gold A, Gabet Y, Bab I, et al: Prediction of fracture callus mechanical properties using micro-CT images and voxel-based finite element analysis. *Bone* 36: 480–488. <https://doi.org/10.1016/j.bone.2004.11.007>, 2005
- Swain MV, Xue J: State of the art of micro-CT applications in dental research. *Int J Oral Sci* 1(4): 177–188. <https://doi.org/10.4248/ijos09031>, 2009
- Ulrich D, van Rietbergen B, Laib A, Rueggsegger P: The ability of three-dimensional structural indices to reflect mechanical aspects of trabecular bone. *Bone* 25(1): 55–60. [https://doi.org/10.1016/s8756-3282\(99\)00098-8](https://doi.org/10.1016/s8756-3282(99)00098-8), 1999

- Umoh JU, Sampaio AV, Welch I, Pitelka V, Goldberg HA, Underhill TM, et al: In vivo micro-CT analysis of bone remodeling in a rat calvarial defect model. *Phys Med Biol* 54(7): 2147–2161. <https://doi.org/10.1088/0031-9155/54/7/020>, 2009 Epub 2009 Mar 13
- Ye JH, Xu YJ, Gao J, Yan SG, Zhao J, Tu Q, et al: Critical-size calvarial bone defects healing in a mouse model with silk scaffolds and SATB2-modified iPSCs. *Biomaterials* 32(22): 5065–5076. <https://doi.org/10.1016/j.biomaterials.2011.03.053>, 2011 Epub 2011 Apr 13
- Zhang ZY, Teoh SH, Chong MS, Lee ES, Tan LG, Mattar CN, et al: Neo-vascularization and bone formation mediated by fetal mesenchymal stem cell tissue engineered bone grafts in critical-size femoral defects. *Biomaterials* 31(4): 608–620. <https://doi.org/10.1016/j.biomaterials.2009.09.078>, 2010